# Optical vibrons in CdSe dots and dispersion relation of the bulk material

C. Trallero-Giner,* A. Debernardi, and M. Cardona
*Max-Planck-Institut für Festkörperforschung, Heisenbergstrasse 1, D-70569 Stuttgart, Germany*

E. Menéndez-Proupín
*Deptartment of Theoretical Physics, Havana University, Vedado 10400, Havana, Cuba*

A. I. Ekimov
*Ioffe Physicotechnical Institute, St. Petersburg, 194021, Russia*
(Received 26 August 1997)

We examine the dependence on size distribution of the Raman line shape of optical vibron modes in CdSe dots. A detailed comparison with the theory of electron-hole correlated Raman scattering in spherical quantum dots, which includes LO-confined modes, is carried out. The obtained CdSe vibron frequencies are found to map well on the *ab initio* calculated LO phonon dispersion relations of wurtzite CdSe along the [001] direction of the Brillouin zone. [S0163-1829(98)06808-8]

## I. INTRODUCTION

Investigations of the quasi-zero-dimensional heterostructures or quantum dots (QD's) have been carried out in particular for II-VI semiconducting compounds.[1] Today, several advanced techniques[2] make it possible to grow size selected II-VI quantum dots with spherical shape, normally embedded in a glass matrix. The vibrational modes and the electron optical-vibron interaction of these systems are objects of study due to the interest in the linear and nonlinear optical properties, Raman scattering, and other effects.[1] The understanding of the lattice dynamical properties and electron optical vibrational mode interaction of these II-VI low-dimensional heterostructures starts with an adequate knowledge of their bulk phonon dispersion. Unfortunately, the literature is scarce in bulk phonon dispersion data for many of the Cd-VI compounds, the main reason being that inelastic neutron scattering cannot be performed due to the large neutron capture cross section of $^{113}$Cd present in natural Cd.[3]

Raman scattering allows a semiquantitative determination of bulk optical branches by measuring the mode frequencies $\omega_n$ as a function of QD radius. For this purpose, the optical vibrations are considered to be confined to the dots with spherical shape and are assigned an equivalent wave vector[4]

$$q_n=\frac{\mu_n}{R}, \tag{1}$$

where $\mu_n$ is the $n$th node of the spherical Bessel function $j_1$ and $R$ the QD radius. A similar method has been successfully applied to determine LO and TO bulk phonon dispersion relations along different crystal directions by studying the confined optical phonons in short period quasi-one-dimensional GaAs/AlAs superlattices.[5–7]

A direct determination of the mode frequencies and the equivalent wavevectors from the Raman spectrum in CdSe QD's appears to be more complex because of the size distribution of the dots embedded in the matrix. In addition, under normal growth conditions the CdSe QD's have the wurtzite (hexagonal) structure[2] and the crystallographic axes of the nanocrystallites are randomly orientated in the glass matrix. In fact, a detailed comparison with the theory of the Raman line shape in QD semiconductors, including exciton-optical vibron interaction, becomes necessary in order to extract meaningful information on bulk phonon frequencies from the observed Raman spectra of nanocrystallites.

We have recently developed a formalism for calculating first order Raman scattering by spherical semiconductor nanostructures. In this formalism, the Fröhlich interaction with optical vibrational modes is treated within a continuum model which takes into account both the elastic and the dielectric properties of the dot.[4,8,9] Neglecting valence band mixing at the $\Gamma$ point of the Brillouin zone, and in the dipole approximation, it is shown that in the Raman process only excitonic states and vibrational modes with zero angular momentum are allowed.[9] Assuming a quadratic negative bulk LO-phonon dispersion the vibron eigenfrequencies are given by

$$\omega_n^2=\omega_L^2-\beta_L^2\left(\frac{\mu_n}{R}\right)^2, \tag{2}$$

where $\omega_L$ is the bulk LO phonon frequency at the Brillouin zone center and $\beta_L$ a parameter describing the dispersion of the LO phonon in the bulk. Using Eqs. (1) and (2), and the dependence on size distribution of the observed Raman spectra of nanocrystallites we should, in principle, be able to derive the average of the LO-phonons dispersion relation in CdSe.

In this paper we show that the model outlined in Refs. 8,9, together with *ab initio* phonon dispersion calculations, leads to an understanding of the principal features of the Raman spectra of QD's in CdSe. We first present a detailed analysis of the Raman line shape in terms of size distribution, phonon linewidths, and photon energy of the exciting laser, whereby

 

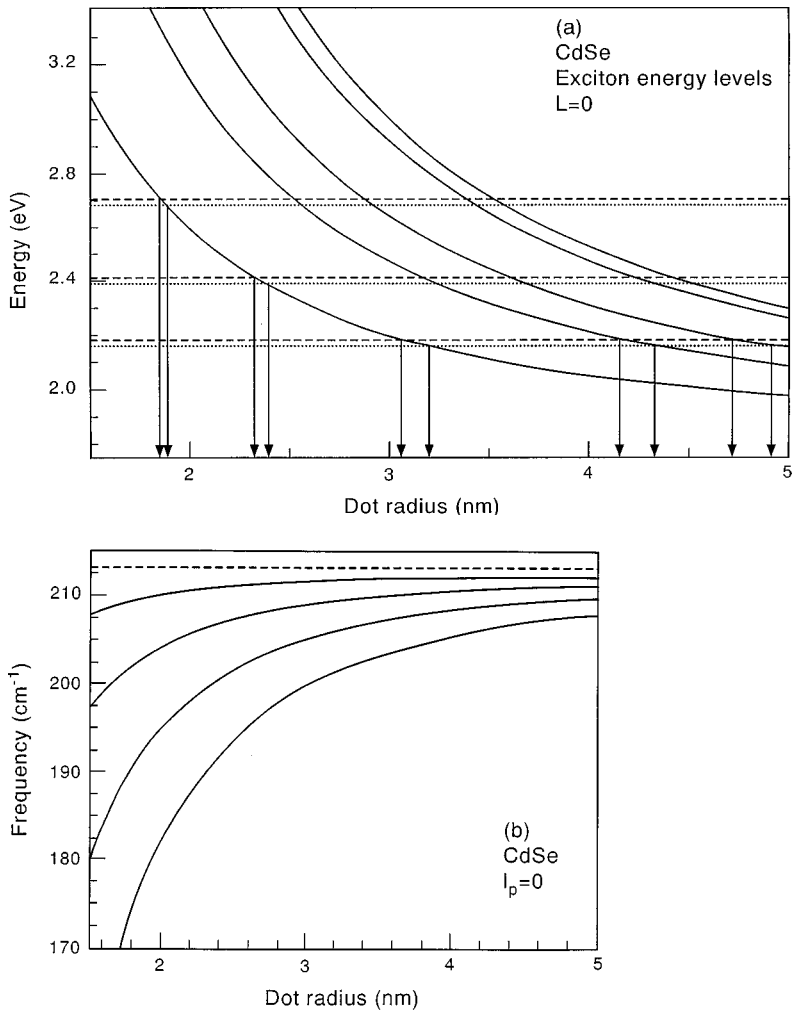


FIG. 1. The radial dependence of the exciton energy levels for $L=0$ (a) and the $l_p=0$ optical-vibron modes (b) for a CdSe spherical quantum dot embedded in a glassy matrix. In the calculation the parameters of Table I have been used. In (a) the excitation laser energies and the corresponding outgoing scattered energies used for the spectra of Figs. 3 are shown by dashed lines and dotted lines, respectively. The resonance radii for several excitonic states are indicated by arrows.

we stress the role of the excitonic states in resonance with the incoming and scattered light in the observed Raman spectra. We show that the asymmetric broadening observed in the Raman line shape with decreasing mean quantum dot radius is due to the contribution of a distribution of vibron modes selected by the resonance of the exciting laser and the scattered light with the confined excitonic states. Comparison of the theoretical results with the measured dependence of the Raman spectra on the size distribution of the QD brings forth the vibron frequencies as a function of QD radius. We compare them with the corresponding bulk LO-phonon dispersion obtained by *ab initio* lattice dynamical calculations. With this method, and the available samples, it is possible to explore dispersion relations of bulk phonons in CdSe up to 50% into the Brillouin zone.

## II. THEORETICAL BACKGROUND

The average Raman cross section of an ensemble of spherical quantum dots with a size distribution function $F(R)$ can be expressed as

$$\left\langle \frac{\partial^2\sigma}{\partial\Omega\,\partial\omega_s} \right\rangle = \int F(R)\,\frac{\partial^2\sigma}{\partial\Omega\,\partial\omega_s}(R;\omega_l,\boldsymbol{e}_l;\omega_s,\boldsymbol{e}_s)\,dR, \quad (3)$$

where the cross section of the single QD of radius $R$ per unit solid angle $d\Omega$ and per unit scattered light frequency $d\omega_s$ for incoming light frequency $\omega_l$ is given by[8,9]

$$\frac{\partial^2\sigma}{\partial\Omega\,\partial\omega_s} = S_0 \sum_n \left| \sum_{\mu_1,\mu_2} \frac{\langle F|H^+_{E-R}|\mu_2\rangle\langle\mu_2|H_{E-V}|\mu_1\rangle\langle\mu_1|H^-_{E-R}|I\rangle}{[\hbar\omega_s - E_{\mu_2}(R)+i\Gamma_{\mu_2}][\hbar\omega_l - E_{\mu_1}(R)+i\Gamma_{\mu_1}]} \right|^2 \frac{\Gamma/\pi}{[\hbar\omega_l-\hbar\omega_s-\hbar\omega_n(R)]^2+\Gamma^2}. \quad (4)$$

TABLE I. Values of the material parameters used for the numerical calculations. Here $m_e$ and $m_h$ are the electron hole effective mass, respectively, $m_0$ is the bare electron mass, $E_g$ is the bulk band gap and $\varepsilon_0$ the static dielectric constant.

| Parameters | CdSe |
|---|---|
| $E_g$ (eV) | 1.865[a] |
| $\omega_L$ ($cm^{-1}$) | 213.1[b] |
| $m_e/m_0$ | 0.12[c] |
| $m_h/m_0$ | 0.44[c] |
| $\beta_L$ ($ms^{-1}$) | $2.969\times10^3$ [b] |
| $\epsilon_0$ | 9.53[d] |
| $a$ (nm) | 0.42999[c] |
| $c$ (nm) | 0.70109[c] |

[a]Reference 15.
[b]Reference 16.
[c]Reference 17.
[d]Reference 18.

The final state $|F\rangle$ of the system consists of single vibrons of frequency $\omega_n(R)$ [statistically created following the distribution function $F(R)$] and a photon of frequency $\omega_s$. $|\mu_i\rangle$ ($i=1, 2$), refers to the intermediate excitonic states, with energy $E_{\mu_i}(R)$ and lifetime broadening $\Gamma_{\mu_i}$. In Eq. (4) $H^+_{E\text{-}R}$ ($H_{E\text{-}V}$) is the crystal-radiation (exciton-vibron) interaction, $S_0$ is a constant involving physical parameters,[9] and a Lorentzian function is included in order to take into account the vibron linewidth $\Gamma$. Details of the scattering efficiency calculation considering either free electron-hole pairs or excitons as intermediate states of the QD can be seen elsewhere.[8,9] The resonant character of the Raman process is evidenced by the denominators which appear in Eq. (4). Incoming resonance takes place when the energy of the laser photon coincides with one of the exciton energies $E_{\mu_1}$ while outgoing resonance occurs when the scattered frequency equal $E_{\mu_2}$.[10] Assuming an ensemble of spherical dots with a size distribution, the conditions $\hbar\omega_l = E_{\mu_1}(R)$ or $\hbar\omega_l - \hbar\omega_n(R) = E_{\mu_2}(R)$ select the Raman spectra of a set of quantum dots with radii $\{R_i\}$ in either incoming or outgoing resonance. In the following, a precise determination of the resonance dot radii $R_i$ becomes necessary to evaluate the equivalent wave vectors $q_n$ involved in the measured Raman spectra. In our case the energy of the exciton ground state has been fitted as a function of the mean radius to the experimental energy of the $N=1$ exciton state obtained from absorption measurements at 4.2 K using an effective radius (in nm) $R_{ef} = 3.367 + 0.90785\ R$ (the constant term 0.336 should account for possible inaccuracies in the $R$ determination or in the boundary conditions).[2] In Fig. 1(a), we illustrate the allowed exciton energies calculated for the first five $L=0$ levels of CdSe nanocrystals embedded in a glassy matrix. The calculation has been performed as discussed in Ref. 9, using the material parameters given in Table I. The dot radii for certain incoming (dashed lines) and outgoing (dotted lines) resonance energies are shown by pairs of arrows. These ''resonant'' dots give the main contribution to the Raman line shape, thus selecting those vibrational modes with frequencies $\omega_n(\mu_n, R_i)$ which fulfill a resonance condition. The optical vibrational energies of the first four $l_p=0$ modes in a spherical CdSe are shown in Fig. 1(b) as a function of $R$.

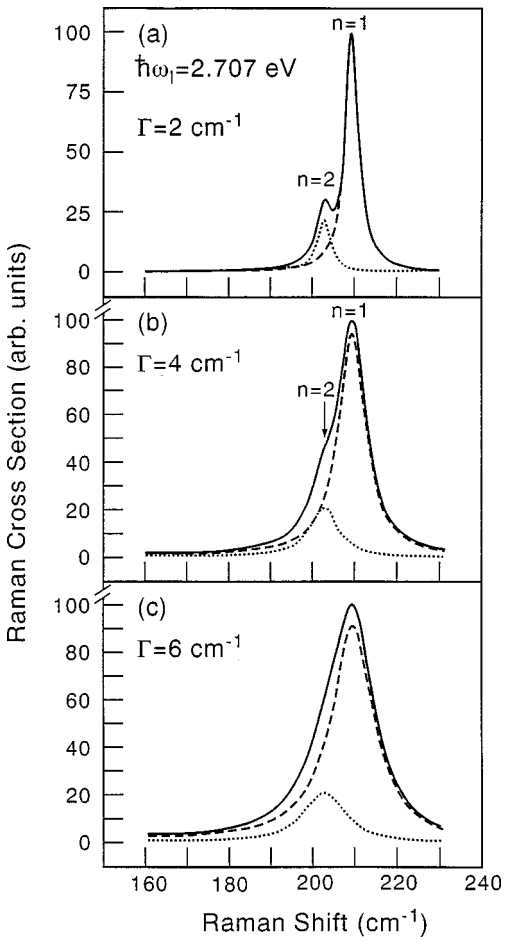


FIG. 2. Raman cross section as a function of Stokes shift for a 1.8 nm radius CdSe sphere embedded in glass at $\hbar\omega_l = 2.707$ eV and different vibron broadening. (a) $\Gamma = 2\ cm^{-1}$, (b) $\Gamma = 4\ cm^{-1}$, and (c) $\Gamma = 6\ cm^{-1}$. The contributions of $l_p=0$, $n=1$, and $l_p=0$, $n=2$ vibron modes to the total line shape are displayed by dashed and dotted lines, respectively.

Let us now analyze the Raman spectrum in terms of the size distribution of quantum dots. The relative contribution of the excitonic and vibronic states to the Raman line shape depends on the incoming laser frequency, the excitonic oscillator strength, and the exciton-vibron interaction. According to Fig. 1(b), vibrons with different quantum number $n$ are expected to play a role in the scattering process, especially when the resonance condition selects small radii, and broadening and asymmetry of the Raman spectrum follow from the contribution of several vibron modes evaluated at different radii in the resonance regime. The main contribution to the Raman spectrum comes from QD's with radii in the range $|R_e - R| < \delta R$, where $R_e$ denotes the radius for which either incoming or outgoing resonance is reached. An estimation of $\delta R$ can be obtained with the following equation:

$$\Gamma_\mu = \frac{\partial E_\mu(R)}{\partial R}\,\delta R. \tag{5}$$

Equation (5) represents deviations from resonance equal to the exciton lifetime broadening. For $\Gamma_\mu = 5$ meV and the

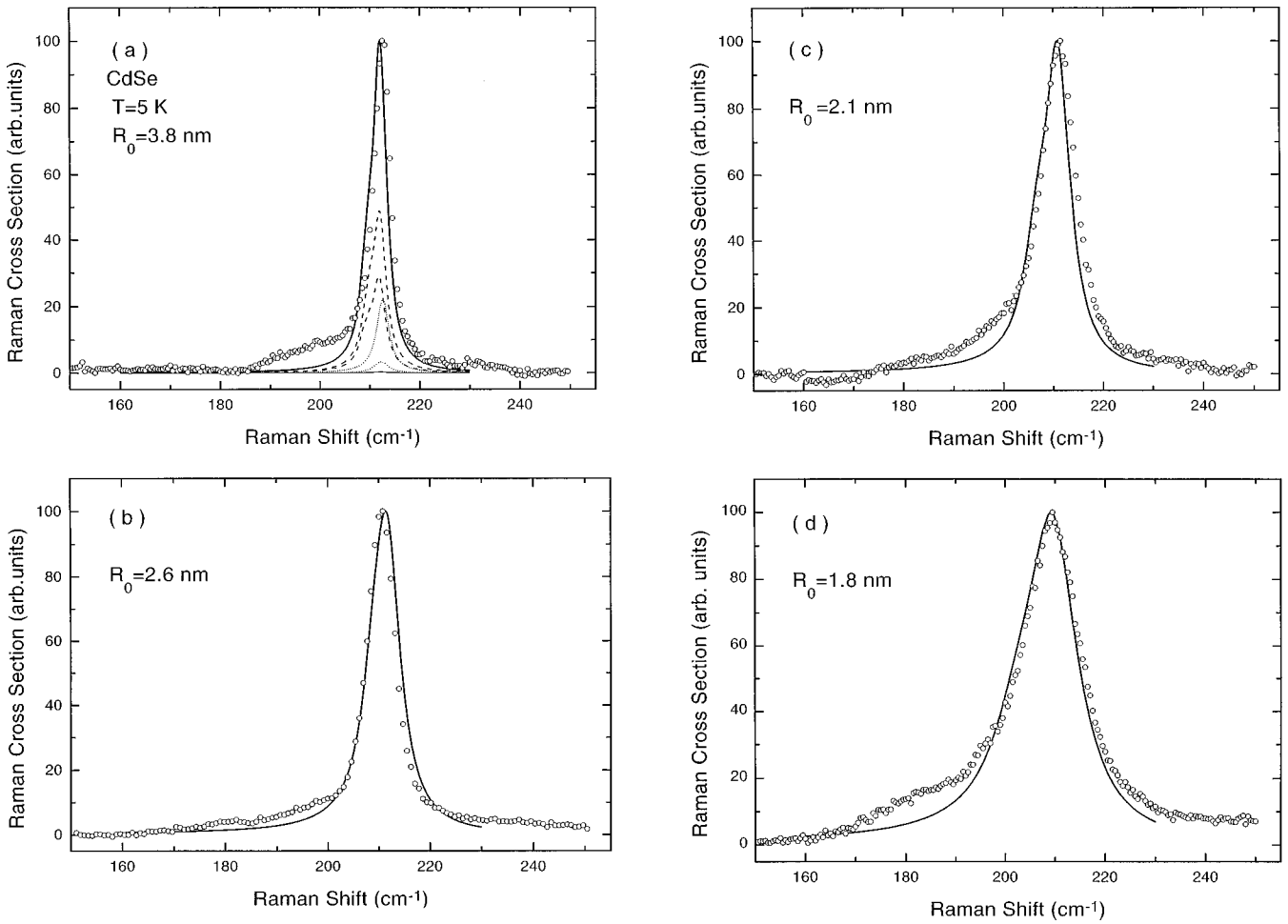


FIG. 3. Raman line shapes for 3.8, 2.6, 2.1, and 1.8 nm mean radius CdSe nanocrystals in a glass matrix measured at 5 K (open dots). The excitation energies are (a) 2.182 eV, (b) 2.182 eV, (c) 2.412 eV, and (d) 2.707 eV. The thick solid lines correspond to the numerical evaluation of Eqs. (2) and (3) following the model of Refs. 4,8,9. The parameters of Table I and a vibron broadening $\Gamma=1.5$, 3, 3, and 6 $\mathrm{cm}^{-1}$ have been used for the fit of spectra (a), (b), (c), and (d), respectively. The different exciton contributions to the calculated line shape are shown in (a). Dashed line: $N=1$ excitonic state; dotted line: $N=3$ excitonic state; and solid line: $N=2$ excitonic state.

material parameters of Table I a maximum value of $\delta R \approx 0.03$ nm is obtained with Eq. (5). The frequency uncertainty for the corresponding single vibron $\delta\omega$ can be cast into the form

$$\frac{\delta\omega}{\omega}=\frac{1}{(\omega_L R/\beta_L\mu_n)^2-1}\,\frac{\delta R}{R} \tag{6}$$

giving an inhomogeneous broadening of $\delta\omega \approx 0.1$ $\mathrm{cm}^{-1}$ for $\delta R=0.02$ nm, $R=2$ nm, and using the parameters of Table I. Figure 2 shows the calculated Raman spectra for different vibron broadenings $\Gamma$. For this calculation we have considered an ensemble of CdSe quantum dots described by a Gaussian size distribution function centered at the mean radius $R_0=1.8$ nm and a dispersion (at half maximum) of $\pm 15\%$. These spectra were obtained for the laser energy $\hbar\omega_l=2.707$ eV, adding up in Eq. (4) the first 10 excitonic levels with $L=0$ for the optical vibrational modes with $n=1$, 2, 3, and 4, using the parameters of Table I. A lifetime broadening $\Gamma_\mu=5$ meV was assumed for all excitonic transitions. The spectra for $\hbar\omega_l=2.707$ eV shown in Fig. 2 correspond to an incoming resonance with the lowest exciton state for a QD with a radius of 1.85 nm, while the outgoing condition determines a maximum resonance radius of 1.88 nm. The Raman line shapes are almost exclusively due to exciton-vibron interaction with the $l_p=0$, $n=1$ and 2 vibron modes, the $l_p=0$, $n=3$ and 4 contributions are too small to be seen in the scale of the figures. The spectrum of Fig. 2(a) which corresponds to a vibron linewidth of $\Gamma=2$ $\mathrm{cm}^{-1}$, shows two well defined peaks related to the $l_p=0$, $n=1$ and a small one related to $l_p=0$, $n=2$ vibrons. Their relative contributions are determined by the $n$-dependent part of the exciton-vibron matrix elements[9] which drop off rapidly with increasing $n$. The Raman spectrum for $\Gamma=4$ $\mathrm{cm}^{-1}$ [Fig. 2(b)] shows, beside the principal structure at 210 $\mathrm{cm}^{-1}$ ($l_p=0$, $n=1$), a shoulder at 203 $\mathrm{cm}^{-1}$ due to the $n=2$ vibron. As the intrinsic vibron linewidth increases, the calculated spectrum [Fig. 2(c) for $\Gamma=6$ $\mathrm{cm}^{-1}$] exhibits an asymmetric broadening towards the low-frequency side, which results from the negative dispersion of the vibron frequencies with increasing radius [see Fig. 1(b)].

## III. RAMAN LINE SHAPE AND OPTICAL VIBRONS

Figures 3(a)–3(d) show four Raman spectra measured at $T=5$ K in CdSe nanocrystals with mean radius $R_0=3.8$, 2.6,

2.1, and 1.8 nm (open dots). The samples were prepared in a borosilicate matrix by a diffusion controlled process (details of the growth procedure are given in Ref. 11). The size dependence of the spectra in Figs. 3(a)–3(d) involves a decrease of the optical mode frequency as well as a broadening of the Raman lines with decreasing QD size. Moreover, the line shapes show an asymmetrical broadening towards the low-frequency side for nanocrystals with $R_0=2.1$ and 1.8 nm.

The calculated Raman cross sections are represented in Figs. 3(a)–3(d) by thick solid lines. The spectrum of Fig. 3(a) corresponds to $\hbar\omega_l=2.182$ eV which is in incoming resonance with the $L=0$, $N=1$, 2, and 3 excitonic states for QD radii equal to 3.1, 4.1, and 4.7 nm, respectively [see Fig. 1(a)]. These excitonic states are in outgoing resonance, calculated with the bulk LO phonon frequency $\omega_L$, for nanocrystal radii $R_e=3.2$, 4.3, and 4.9 nm, respectively. The scattering profiles related to outgoing and incoming resonances with the excitonic states $N=1$, 2, and 3 are shown in Fig. 3(a) by dashed, dotted, and thin lines, respectively. The main contribution comes from the $N=1$ state in outgoing resonance, while the excited state $N=3$ presents an incoming resonance stronger than the outgoing one. The contribution of the $N=2$ state is negligible, its optical oscillator strength being much weaker than those of the $N=1$ and 3 excitonic states.[9] In all analyzed nanostructures the stronger exciton-vibron matrix elements correspond to the $l_p=0$, $n=1$, and $n=2$ vibron modes. In the case of Fig. 3(a) the line shape is a Lorentzian because the resonance radii select vibron modes which are very close in energy. For the calculation of Fig. 3(a) a vibron linewidth $\Gamma=1.5$ cm$^{-1}$ was used. The spectrum for $\hbar\omega_l=2.182$ eV [Fig. 3(b)] in a nanocrystal with a mean radius $R_0=2.6$ nm presents a line shape shifted to lower frequency and somewhat broader than that of the $R_0=3.8$ nm QD. For the case of $\pm 15\%$ size dispersion considered here, contributions from the resonance radius $R_e=4.1$, 4.7 nm and beyond are attenuated by the Gaussian functions centered at $R_0=2.6$ nm. The measured spectrum in Fig. 3(c) was taken at $\hbar\omega_l=2.412$ eV in QD's with $R_0=2.1$ nm. Resonance with the $N=1$ excitonic state is achieved for $R_e=2.3$ and 2.4 nm [see Fig. 1(a)]. Consequently, the corresponding vibron modes are separated sufficiently in frequency [see Fig. 1(b)] for an asymmetrical broadening on the low-frequency side to appear in the calculated Raman scattering efficiency. As the mean radius of the QD's is reduced ($R_0=1.8$ nm) the $l_p=0$ vibron modes are well defined in frequency and the calculated Raman cross section for $\hbar\omega_l=2.707$ eV shows a pronounced asymmetrical spectral line [Fig. 3(d)]. Vibronic linewidths of 3, 3, and 6 cm$^{-1}$ have been used in the calculated spectra of Figs. 3(b), 3(c), and 3(d), respectively. Once again, we have included the $l_p=0$, $n=3$, 4 vibron modes but since their exciton-vibron matrix elements are much smaller, these do not show up in Fig. 3.

The above procedure provides the possibility to evaluate vibrational optical frequencies and their equivalent ''wave vectors'' relevant to the observed Raman spectra. From the fits of Figs. 3 the optical frequencies are obtained in terms of the $n$th mode and radius. In Fig. 4 we plot the LO frequencies obtained for CdSe as described above from the scattering line shape of the four samples of Fig. 3. The corresponding ''wave vectors'' $q_n$ are evaluated using Eq. (1) for each set of ''resonant'' dots. We have also displayed the LO phonon dispersion of bulk CdSe along the main direction of the Brillouin zone ([100], [010], [001]), computed within the mass approximation, from *ab initio* force constants. This approximation is based on the transferability of the electronic force constants computed for one material into another which differs from it basically only by a change in atomic masses. This approximation has been successfully used in the computation of phonon branches in zinc-blende semiconductors with a similar lattice parameter.[12] Our force constants were obtained using density functional perturbation theory[13] for the case of wurtzite CdS.[3] The dispersion relations displayed in Fig. 4, were obtained from the force constants of CdS after replacing in the dynamical equation the mass of S by that of Se. The *ab initio* force constants of CdS have been checked against inelastic neutron scattering measurements.[9] Such measurement are not yet available for CdSe, although there are at present in progress, together with *ab initio* phonon dispersion calculations for a $^{115}$CdSe crystal with the wurtzite structure.

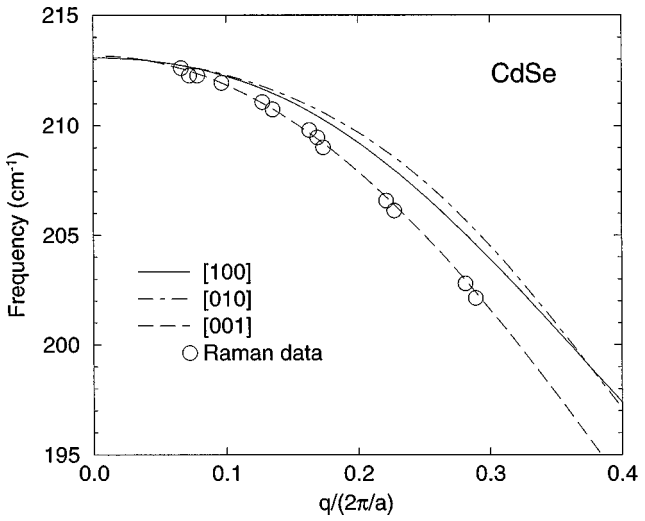


FIG. 4. A plot of the LO-vibron frequencies of CdSe taken from the data of Figs. 3 vs the ''wave vector'' calculated with Eq. (1). The vibrational frequencies have been obtained by comparing of the experimental line shapes of different mean size CdSe nanocrystals with the calculated ones. The curves represent *ab initio* lattice dynamical calculation, within the mass approximation, of the LO-phonon branches wurtzite CdSe along the [100], [010], and [001] directions of the Brillouin zone (see Ref. 16). Note the excellent agreement between the experimental data and the dispersion along [001] (the hexagonal axis).

The somewhat different size of the unit cells of CdS and CdSe is taken into account by writing the reciprocal lattice vectors in reduced units ($2\pi/c$ for [001], $2\pi/a$ for [100] and [010], where $c$ and $a$ are the parameters of the hexagonal unit cell) and using the experimental lattice constants given in Table I. We obtain a LO frequency at the Brillouin zone center of 235 cm$^{-1}$ which is $\sim 10\%$ higher than the experimental one. We therefore scale all the computed frequencies in the Brillouin zone by a constant factor to reproduce the experimental frequency of 213.1 cm$^{-1}$ at the zone center.

The dispersion computed from the experimental data reported here according to the procedure described above are

in good agreement with the calculations of the for [001] bulk phonon dispersion obtained with the mass approximation. We do not find any explanation as to why the frequencies measured through the Raman spectra of QD's embedded in a glass matrix, map so well onto the LO-phonon dispersion along the [001] direction of the Brillouin zone as opposed to the perpendicular directions.

## IV. CONCLUSIONS

In summary, we have carried out a detailed analysis of the Raman spectra in CdSe dots with mean radii between 1.8 and 3.8 nm. We have shown that the main contribution to the observed cross section arises from those microcrystallites in the sample whose sizes favor incoming and outgoing resonances. The $n=1$ and $n=2$ vibron states yield the main contribution to all studied Raman spectra. The shifts and asymmetric broadenings towards the low-frequency side, observed as $R_0$ decreases, are explained by the contribution of different vibron states to the line shape and the negative LO dispersion law [Eq. (2)] of CdSe. To fit the spectra of Figs. 3 the phenomenological vibron linewidths $\Gamma$ should increase as $R_0$ is reduced. This can be attributed to several causes

(i) The mixing effects of the hole subbands allows the exciton-vibron interaction with $l_p=2$ modes including the so-called surfacelike modes.[14]

(ii) Dots with nonspherical shapes should relax the $L=0$ and $l_p=0$ selection rules, the frequency modes with $l_p\neq 0$, disallowed for perfect nanospheres, should contribute to the broadening of the Raman spectra.

(iii) Defects or impurities in the dots induce Raman scattering with the participation of $l_p=1$ vibronic modes.

The broad shoulders seen at the low-frequency side of the main peak on the spectra of Figs. 3 can be qualitatively explained by the relaxation of the $l_p=0$ selection rule. These shoulders are centered around 190 $cm^{-1}$ and move to lower energies as the mean radius decreases. An evaluation of the $l_p=1$ modes for CdSe nanospheres reveals a mode at 189.5 $cm^{-1}$ (the so-called Fröhlich mode). Those resonance radii which pick up frequencies around the Fröhlich frequency select optical vibrations which have a strong electrostatic contribution and, in this way, strong exciton-vibron interaction can be achieved.

Finally, the optical vibron frequencies obtained by the fitting procedure described above can be mapped using the wave vector given in Eq. (1) onto *ab initio* lattice dynamics calculations for wurtzite CdSe. The obtained frequencies map well onto the LO-phonon dispersion along the [001] direction of the Brillouin zone. Our results are consistent with a negative parabolic dispersion law for the bulk LO phonons, with a phenomenological parameter $\beta_L$ equal to $2.989\times 10^3$ m/sec, which applies at least over the first half of the bulk Brillouin zone of CdSe.

## ACKNOWLEDGMENTS

We would like to thank A. A. Sirenko for a critical reading of the manuscript. C. Trallero-Giner is grateful to the Max-Planck-Institut für Festkörperforschung for its hospitality.

*Also at Dept. of Theoretical Physics, Havana University, Vedado 10400, Havana, Cuba.

[1] C. W. J. Beenakker and H. van Houten, in *Solid State Physics: Semiconductor Heterostructures and Nanostructures*, edited by H. Ehrenreich and D. Turnbull (Academic, San Diego, 1991), Vol. 44.

[2] A. Ekimov, J. Lumin. **70**, 1 (1996).

[3] A. Debernardi, N. M. Pyka, A. Göbel, T. Ruf, R. Lauck, S. Kramp, and M. Cardona, Solid State Commun. **103**, 297 (1997).

[4] E. Roca, C. Trallero-Giner, and M. Cardona, Phys. Rev. B **49**, 13 704 (1994).

[5] A. K. Sood, J. Menéndez, M. Cardona, and K. Ploog, Phys. Rev. Lett. **54**, 2111 (1985).

[6] Z. V. Popović, M. Cardona, E. Richter, D. Strauch, L. Tapfer, and K. Ploog, Phys. Rev. B **41**, 5904 (1990).

[7] D. J. Mowbray, M. Cardona, and K. Ploog, Phys. Rev. B **43**, 1598 (1991).

[8] M. P. Chamberlain, C. Trallero-Giner, and M. Cardona, Phys. Rev. B **51**, 1680 (1995).

[9] E. Menéndez, C. Trallero-Giner, and M. Cardona, Phys. Status Solidi B **199**, 81 (1997).

[10] M. Cardona, in *Light Scattering in Solids II*, Vol. 50 of *Topics in Applied Physics*, edited. by M. Cardona and G. Güntherodt (Springer-Verlag, Heidelberg, 1982), p. 19.

[11] L. Saviot, B. Champagnon, E. Duval, I. A. Kudriavtsev, and A. I. Ekimov, J. Non-Cryst. Solids **197**, 238 (1996).

[12] S. Baroni, P. Giannozzi, and A. Testa, Phys. Rev. Lett. **58**, 1861 (1987).

[13] P. Giannozzi, S. de Gironcoli, P. Pavone, and S. Baroni, Phys. Rev. B **43**, 7231 (1990).

[14] A. L. Efros, A. I. Ekimov, F. Kozlowski, V. Petrova-Koch, H. Schmidbauer, and S. Shumilov, Solid State Commun. **78**, 853 (1991).

[15] The best fit obtained from the fundamental absorption optical transition as a function of QD's radii after Ref. 2. The size dependence of excitonic optical transitions energy measured in CdSe dots in a glass matrix[2] does not exhibit any evidence of the *A*- and *B*-excitonic structure due to crystalline field splitting of valence band presents in wurtzite CdSe. In our calculation one excitonic band mode is used, while the observed experimental energy of the first optical transition is fitted to the energy of the exciton ground state as a function of radius.

[16] Obtained by fitting with Eq. (2) the maxima of the Raman spectra as a function of the nanocrystals mean radii. The *ab initio* calculated value is $\omega_L=235.4$ $cm^{-1}$. It has been scaled, as with all the curves in Fig. 4 so as to fit the experimental $\omega_L=213.1$ $cm^{-1}$.

[17] U. Rössler, in Landolt-Börnstein *Numerical Data and Functional Relationships in Science and Technology*, edited by O. Madelung, H. Schulz, and H. Weiss (Springer, Berlin, 1987), Vol. III/22a, p. 204.

[18] R. G. Alonso, E. Suh, A. K. Ramdas, N. Samarth, H. Luo, and J. K. Furdyna, Phys. Rev. B **40**, 3720 (1989).